

RNA secondary structure regulates the translation of *sxy* and competence development in *Haemophilus influenzae*

Andrew D.S. Cameron^{1,2}, Milica Volar², Laura A. Bannister² and Rosemary J. Redfield^{2,*}

¹Department of Microbiology and Immunology and ²Department of Zoology, University of British Columbia, Vancouver, British Columbia, Canada

Received August 24, 2007; Revised October 4, 2007; Accepted October 7, 2007

ABSTRACT

The *sxy* (*tfoX*) gene product is the central regulator of DNA uptake by naturally competent γ -proteobacteria such as *Haemophilus influenzae*, *Vibrio cholerae* and probably *Escherichia coli*. However, the mechanisms regulating *sxy* gene expression are not understood despite being key to understanding the physiological role of DNA uptake. We have isolated mutations in *H. influenzae sxy* that greatly elevate translation and thus cause competence to develop in otherwise non-inducing conditions (hypercompetence). *In vitro* nuclease analysis confirmed the existence of an extensive secondary structure at the 5' end of *sxy* mRNA that sequesters the ribosome-binding site and start codon in a stem-loop. All of the hypercompetence mutations reduced mRNA base pairing, and one was shown to cause a global destabilization that increased translational efficiency. Conversely, mutations engineered to add mRNA base pairs strengthened the secondary structure, resulting in reduced translational efficiency and greatly reduced competence for genetic transformation. Transfer of wild-type cells to starvation medium improved translational efficiency of *sxy* while independently triggering the sugar starvation regulator (CRP) to stimulate transcription at the *sxy* promoter. Thus, mRNA secondary structure is responsive to conditions where DNA uptake will be favorable, and transcription of *sxy* is simultaneously enhanced if CRP activation signals that energy supplies are limited.

INTRODUCTION

Natural competence, the ability to take up DNA molecules directly from the environment, is tightly

regulated in most bacteria, indicating that the costs and benefits of DNA uptake depend on changes in the extracellular and intracellular environments. Because the mechanisms regulating competence evolved to allow cells to track these changes, understanding the mechanisms provides a window on the importance of DNA uptake to the cell.

Bacteria in the families *Pasteurellaceae*, *Enterobacteraceae* and *Vibrionaceae* appear to share a common regulatory mechanism, with competence genes organized in a regulon whose transcription is controlled by two activator proteins, Sxy (also known as TfoX) and CRP (also known as CAP) (1). Although competence genes are ubiquitous in these families, only a few species are known to be naturally competent, and the only well-studied competence regulon is that of *Haemophilus influenzae* (*Pasteurellaceae*). *H. influenzae* becomes moderately competent as growth slows during late log phase in rich medium, and becomes maximally competent when log phase cells are transferred to the defined starvation medium MIV (2).

The *sxy* gene was first identified and named as the site of the *H. influenzae* mutation *sxy-1*, which causes greatly increased competence (hypercompetence) during growth in rich medium (3). Cells lacking *sxy* cannot induce the 25 genes (13 transcription units) of the competence regulon; many of these genes are known to contribute directly to DNA uptake (2). Conversely, overexpression of *sxy* from multi-copy plasmids induces competence under what are normally non-inducing conditions in *H. influenzae*, *Actinobacillus actinomycetemcomitans* and *Vibrio cholerae* (4–6). Unlike Sxy, CRP is a global regulator. It activates a broad array of genes united by their roles in obtaining or utilizing alternative carbon or energy sources, or in sparing the wasteful use of the preferred sources; its action has been very well studied in *Escherichia coli*. When activated by its allosteric effector cyclic AMP (cAMP), CRP binds specifically to 22 bp sites in promoters where it stimulates transcription. Competence regulon promoters contain a novel type of

*To whom correspondence should be addressed. Tel: +604 822 3744; Fax: +604 827 4135; Email: redfield@zoology.ubc.ca

Table 1. Strains used in this work

Strain or plasmid	Relevant genotype	Source or reference
<i>H. influenzae</i>		
KW20	Wild-type Rd; Sequenced strain	(37)
MAP7	KW20 Nov ^r	(38)
RR648	KW20 <i>sxy</i> ::Kan ^r	(4)
RR668	KW20 <i>eyaA</i> ::miniTn10kan	(39)
RR699	KW20 <i>sxy</i> -1	(4)
RR700	KW20 <i>sxy</i> -2	This study
RR723	KW20 <i>sxy</i> -3	This study
RR724	KW20 <i>sxy</i> -4	This study
RR844	KW20 <i>sxy</i> ₈₉ :: <i>lacZKan</i> ^r (operon fusion)	This study
RR845	KW20 <i>sxy</i> ₈₉ :: <i>lacZKan</i> ^r (protein fusion)	This study
RR846	KW20 <i>sxy</i> ₁₁ :: <i>lacZKan</i> ^r (operon fusion)	This study
RR847	KW20 <i>sxy</i> ₁₁ :: <i>lacZKan</i> ^r (protein fusion)	This study
RR850	KW20 <i>sxy</i> -5	This study
RR852	KW20 <i>sxy</i> -6	This study
RR854	KW20 <i>sxy</i> -7	This study
<i>E. coli</i>		
DH5α	<i>F80lacZ Δ(lacIZYA-argF) endA1</i>	
JM109	<i>endA1, recA1</i>	Promega
M15	<i>lacZ, pREP4</i>	Qiagen
RR1128	M15 pQE <i>sxy</i>	This study
Plasmids		
pDJM90	UTR and 5'-half of <i>sxy</i> ORF	(4)
pLZK80	<i>lacZKan</i> ^r operon fusion cassette	G. Barcak
pLZK81	<i>lacZKan</i> ^r protein fusion cassette	G. Barcak
pLBSF1	<i>sxy</i> ₈₉ :: <i>lacZKan</i> ^r (operon fusion)	This study
pLBSF2	<i>sxy</i> ₈₉ :: <i>lacZKan</i> ^r (protein fusion)	This study
pLBSF3	<i>sxy</i> ₁₁ :: <i>lacZKan</i> ^r (operon fusion)	This study
pLBSF4	<i>sxy</i> ₁₁ :: <i>lacZKan</i> ^r (protein fusion)	This study
pGEM-7Zf-	T7 promoter	Promega
pGEM <i>sxy</i>	<i>sxy</i> ORF and UTR cloned in pGEM-7Zf-	This study
pGEM <i>sxy</i> -1	<i>sxy</i> -1 ORF and UTR cloned in pGEM-7Zf-	This study
pGEM <i>sxy</i> -7	<i>sxy</i> -7 ORF and UTR cloned in pGEM-7Zf-	This study
pREP4	<i>lacIq</i>	Qiagen
pQE <i>sxy</i>	<i>sxy</i> ORF cloned in pQE-30UA (Qiagen)	This study

Nov^r, novobiocin resistance; Kan^r, kanamycin resistance; Cam^r, chloramphenicol resistance.

CRP site (CRP-S sites, previously called competence regulatory elements), whose sequences differ at critical positions from the canonical CRP sites previously characterized in *E. coli* (CRP-N sites) (1).

Understanding how competence is regulated depends on understanding how both CRP and Sxy are regulated. In *H. influenzae* and in *E. coli*, CRP is activated by a rise in cAMP that occurs when preferred sugars are unavailable for transport by the phosphotransferase system (7,8). We have previously shown that *H. influenzae sxy* mRNA levels rise when cells experience competence-inducing conditions (2), but nothing is known about the molecular events that control this expression.

The original *sxy*-1 mutation causes only a very conservative change in the Sxy protein sequence (Val₁₉Ile), and it was proposed to cause hypercompetence by increasing the amount of Sxy rather than by changing the nature of Sxy's action (4). Here we report the isolation and characterization of additional hypercompetence-causing point mutations in *sxy*, none of which alter the protein sequence. We show that all the hypercompetence mutations act by increasing *sxy* expression, and that this effect arises by destabilization of an mRNA secondary structure that normally limits *sxy* translation in rich medium. In maximal competence-inducing conditions,

CRP induces *sxy*; together CRP and Sxy then induce the genes of the CRP-S regulon.

MATERIALS AND METHODS

Strains, plasmids and DNA

Bacterial strains and plasmids used in this study are listed in Table 1.

Culture conditions and transformation assays

H. influenzae cells were cultured at 37°C in brain heart infusion (BHI) supplemented with NAD (2 µg/ml) and hemin (10 µg/ml) (sBHI), and with novobiocin (2.5 µg/ml), kanamycin (7 µg/ml) or chloramphenicol (2 µg/ml) added when required. Competence was induced by transferring log-phase cells to the defined starvation medium MIV as previously described (9). *E. coli* cells were grown in Luria Bertani (LB) medium, with kanamycin (25 µg/ml) and ampicillin (100 µg/ml) when required.

Competent *H. influenzae* cells were transformed with chromosomal or plasmid DNA as previously described (10). Cells (1 ml) were incubated with 1 µg/ml of MAP7 chromosomal DNA for 15 min, the DNA was degraded by incubation with DNase I for 5 min and cells were diluted

and plated on sBHI agar with and without novobiocin. Transformation frequencies were calculated as the number of novobiocin-resistant (Nov^R) transformants per cell. The *sxy*-2, -3, -4 and -5 mutants were isolated by selection of exponentially growing EMS-mutagenized cells for transformation to Nov^R, as described for *sxy*-1 (3). *E. coli* cells were made chemically competent with RbCl and transformed with plasmids as previously described (11).

Site-directed mutagenesis

The 1.8 kb EcoRI–BamHI fragment of pDJM90 (*sxy*) was cloned into the EcoRI–BamHI site of pAlter-1 (Promega) to create the plasmid pAlter*sxy*. Site-directed mutagenesis was carried out using the Altered Sites II kit (Promega), following the manufacturer's protocol. Sequencing was used to confirm mutations, and the sequenced regions between ScaI–ClaI sites were subcloned into pDJM90 to ensure that the plasmid inserts contained no additional mutations.

Generation of polyclonal anti-Sxy antibodies

The *sxy* coding sequence was cloned under *lac* promoter control in the His-tag vector pQE30-UA (Qiagen) in *E. coli* M15, and *sxy* expression was induced at A₆₀₀ 0.6 with 1 mM IPTG. Cells were harvested after 4.5 h by centrifugation and the pellet was frozen overnight at –20°C. Because Sxy invariably formed inclusion bodies in expression cultures, even when induced with low concentrations of IPTG and at 30°C, it was denatured and purified as follows. The frozen cell pellet was resuspended in lysis buffer (100 mM NaPO₄, 10 mM Tris–HCl, 6 M guanidine HCl, pH 8.0), then cells were incubated 1 h at 30°C with shaking followed by brief, gentle vortexing until the solution was translucent. Cellular debris was removed by centrifugation at 10 000g for 25 min and the supernatant was incubated with nickel-nitriloacetic acid agarose beads for 1 h at 4°C with gentle rocking. Agarose beads were packed in a column and washed twice with 12 column volumes of wash buffer (100 mM NaPO₄, 10 mM Tris–HCl, 8 M urea, pH 6.3), and protein was eluted using 2 vol of wash buffer pH 4.5. Eluted fractions were pooled and concentrated by precipitation with 10% TCA. Residual TCA was removed with cold 100% ethanol, and protein was dried and resuspended in SDS sample buffer (45 mM Tris–HCl pH 7.5, 10% glycerol, 1% SDS, 50 mM DTT, 0.01% bromophenol blue). Proteins were then separated by electrophoresis on a 15% polyacrylamide SDS gel, and the section of gel containing Sxy (MW 25 kDa) was excised and macerated by repeated passage through a small-bore syringe. Protein was eluted overnight in water, and then concentrated by TCA precipitation. Dried protein was resuspended in phosphate-buffered saline (137 mM NaCl, 10 mM phosphate, 2.7 mM KCl, pH 7.4) and purity was assessed with SDS–PAGE and quantified using the Bradford assay. Protein was emulsified in incomplete Freund's adjuvant (250 µg/ml) for injection in rabbits. Blood serum was collected 10 days after booster shots and stored at –20°C until use.

Western blot and spot blot analysis

For western blots, cells were pelleted and resuspended in SDS sample buffer and proteins were separated on 15% polyacrylamide SDS gels. All gels were run in duplicate to provide one gel for western blot analysis and a second for Coomassie staining to confirm that a consistent amount of protein was loaded in each well. Gels were equilibrated in transfer buffer (48 mM Tris–HCl, 39 mM glycine) and proteins were transferred to PVDF membrane at 10 V for 30 min using a Trans-blot semi-dry (Bio-Rad) apparatus. Samples from *in vitro* translation reactions were spotted in duplicate on pre-wetted PVDF membrane; after drying, spotted membranes were re-wetted with methanol then washed with water and TBS-T (20 mM Tris–HCl pH 7.5, 137 mM NaCl, 0.05% Tween-20).

All membranes were blocked overnight at 4°C in 5% non-fat powdered milk in TBS-T, followed by incubation at room temperature for 1 h with rocking in rabbit anti-Sxy serum diluted 1/10 000 in TBS-T (1% blocking agent). Blots were washed thoroughly and probed with alkaline phosphatase-linked anti-rabbit antibody diluted 1/10 000 in TBS-T (1% blocking agent) for 1 h at room temperature with rocking, followed by thorough washing. Blots were incubated in ECF reagent (Amersham) for 1 min. Bands were visualized using a Typhoon 9400 scanner (GE Healthcare) and quantified using Image Quant (GE Healthcare). Several other *H. influenzae* proteins in addition to Sxy were recognized by the polyclonal antiserum in western blots. These unidentified *H. influenzae* proteins were also bound by pre-immune serum, indicating that antigenicity is not an artifact of non-specific binding by anti-Sxy antibodies. The unidentified proteins demonstrated highly consistent abundance in all culture conditions and growth phases and so were used as internal standards for the quantification of Sxy. Sxy protein levels were calculated after subtracting background signal generated by *sxy*[–] cells (western blots) or by *in vitro* transcription/translation reactions lacking template DNA (spot blots).

Template preparation for RNase analysis

Gene sequences used as templates for *in vitro* preparation of mRNAs were cloned adjacent to the T7 promoter of pGEM-7Zf- (Sigma). The 51 nt long *sxy* untranslated region (UTR) together with the full *sxy* coding region (654 nt) was PCR amplified from genomic DNA isolated from *H. influenzae* KW20 and RR699 (*sxy*-1) using primers PR13 5'-AAAGGGCCCCAGAAGTACTTCTA CTGACTC and PR12 5'-CAAGTAAGTTTATTAATAA AAGCTTAAGCAT. Amplicons were digested and cloned into ApaI and EcoRI restriction sites, generating plasmids pGEM*sxy* and pGEM*sxy*-1 in host strain JM109. Because the primer PR13 overlaps one of the *sxy*-7 mutations (Figure 3A), pGEM*sxy*-7 was constructed by site-directed mutagenesis of pGEM*sxy* using a QuikChange site-directed mutagenesis kit (Stratagene).

RNA preparation

Wild-type *sxy*, *sxy-1* and *sxy-7* RNAs were prepared by transcription *in vitro* (MEGAscript T7 kit, Ambion) from plasmids linearized at position 323, resulting in 340 nt long run-off transcripts. RNAs were purified from the transcription mix, first by a DNase treatment using a DNA-Free Kit (Ambion) and next by a spin column (RNA Easy kit, Qiagen) following the manufacturers' instructions. At this point the concentration of each RNA sample was measured by spectrophotometry, and quality and purity were assessed by agarose gel electrophoresis and $A_{260/280}$ ratios. Next, RNAs (~20 pmol) were dephosphorylated in 100 μ l reactions at 37°C for 2 h in reaction buffer using 0.5 U of calf intestinal alkaline phosphatase (Roche). RNAs were recovered by phenol-chloroform purification and ethanol precipitation. Dephosphorylated RNAs (~10 pmol) were labeled in 50 μ l reactions in reaction buffer using 20 U of T4 polynucleotide kinase (BioLabs, New England) and at least 20 pmol of γ - P^{32} ATP (6000 Ci/mmol; GE Amersham) at 37°C for 1 h. Finally, RNAs were purified by a spin column (RNA Easy kit, Qiagen) and eluted in nuclease-free water.

RNA secondary structure mapping

End-labeled RNAs were denatured for 5 min at 95°C, allowed to re-fold for 15 min at 37°C, and partially digested with RNase A (0.005 U/ml) or RNase TI (0.05 U/ml) (both from Ambion), and the resulting fragments were resolved on sequencing gels. Both partially digested RNAs and control RNAs (ladders) were prepared following the manufacturer's directions. Alkaline-digested end-labeled RNA was used as a ladder to assign gel bands to specific residues in the RNA sequence.

After electrophoresis for 3 h at 900 V and 12 mA, gels were dried, exposed to a PhosphorScreen overnight and visualized using a PhosphorImager (Molecular Dynamics). ImageQuant software was used to measure cleavage intensities at each residue position. Positions 78 and 80 were used as standards to normalize cleavage intensities at all other positions because they were consistently strongly cleaved in independent reactions. To calculate fold differences in cleavage intensities between mutant and wild-type RNA, *sxy-1* or *sxy-7* values were divided by wild-type values at each position. At positions where mutant RNAs were more weakly cut than wild-type, wild-type values were instead divided by mutant and then expressed as a negative value.

In silico RNA secondary structure predictions

Mfold (12) was used to predict secondary structure of the full-length *in vitro* *sxy* transcript [comprising pGEM-7Zf- (15 nt), UTR (51 nt) and partial coding region (274 nt) sequences]; default parameters were used.

Construction of β -galactosidase fusions and enzyme assays

To fuse *lacZ* at *sxy* position 317 (codon 89), *lacZkan* cassettes (~4.5 kb) were excised from pLZK80 and pLZK81 with BamHI and ligated to BclI digested pDJM90, generating pLBSF1 and pLBSF2

(Supplementary Figure 1A). To eliminate Stems 1 and 3, PCR was used to create an EcoRI site at position 83 (codon 11) using primers PR6 5'-GAATTCTGTGATTA TATCTGTATTGATG and PR15 5'-AGGGAATTCG CTATCTATATGCTCATCC. The amplicon was then digested with EcoRI and BclI, ligated to *lacZkan* cassettes and cloned into ScaI + BclI-digested pLBSF1 to generate pLBSF3 and pLBSF4 (Supplementary Figure 1B). All gene fusions were transferred to the KW20 chromosome by excision from plasmids with ApaI + BamHI followed by transformation into competent cells, with selection for kanamycin resistance [method described in (9)].

H. influenzae strains containing *lacZ* fusions were grown in sBHI and sampled in duplicate at regular time intervals. For cells in the mid- to late-log phase of growth ($A_{600} \geq 0.5$), 0.1 ml of cells was usually sampled; for cells in the early-log phase of growth, 0.5 ml samples were taken. After sampling, cells were immediately pelleted by centrifugation, supernatants were removed and cell pellets were frozen at -80°C for later assays of β -galactosidase activity (13). Simultaneously, the main cell culture was assayed for A_{600} and, in some cases, for cfu/ml.

In vitro transcription and translation

The *E. coli* S30 extract system for linear templates (Promega) was used for *in vitro* coupled transcription/translation according to the manufacturer's instructions. Plasmid templates (pGEM*sxy*, pGEM*sxy-1*, pGEM*sxy-7*) were isolated using a GenElute plasmid miniprep kit (Sigma) and residual RNases were removed using a GenElute PCR clean-up kit (Sigma). T7 RNA polymerase (1.4 U/ μ l final concentration) was added to reactions and transcription was initiated by addition of template DNA (4.5 nM final concentration). Some reactions also contained the DNA oligonucleotide 5'-AGTCAGTAGAAG TACTTC at 75 μ M final concentration. Reactions were incubated at 25°C and stopped by mixing with 4 vol of ice-cold acetone.

Quantitative PCR measurement of *sxy* transcript

Total RNA was isolated from cultures using RNeasy Mini Kits (Qiagen), and purity and quality were assessed by electrophoresis on 1% agarose (1 \times TAE). RNA was DNase treated twice with a DNA Free kit (Ambion), followed by cDNA synthesis using the iScript cDNA synthesis kit (Bio-Rad). For each PCR primer set, reactions were carried out in duplicate on a 7000 Sequence Detection System (Applied Biosystems) using iTaq SYBR Green Supermix with ROX (Bio-Rad). PCR primers: *sxy*RTF 5'-TGAACCTTTTACAACGAATGAT; *sxy*RTR 5'-ACACAATCTATTACTACGTAAAATCTGATCAG; *mur*GRTF 5'-TGCTTGGGCTGATGTGTTA; *mur*GRTR 5'-TCCCCTGCTGCAATTTTAC. *murG* RNA served as an internal control for each sample because this gene's expression is constant in the culture conditions used in this study (2). Standard curves were generated using five serial 10-fold dilutions of MAP7 chromosomal DNA.

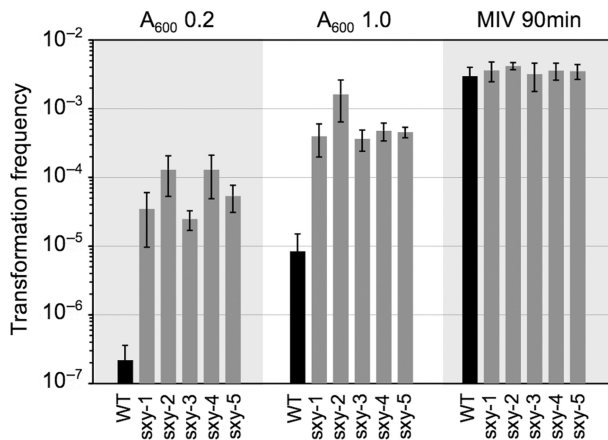


Figure 1. Natural competence assayed by transformation to novobiocin resistance. Transformation frequencies of wild-type (black) and *sxy-1-5* mutants (gray) under non-inducing conditions (log phase: sBHI at A_{600} 0.2), partially inducing conditions (late log: sBHI at A_{600} 1.0) and fully inducing conditions (90 min in MIV).

RESULTS

Isolation and characterization of additional hypercompetence mutations in *sxy*

The original *sxy-1* hypercompetent mutant was isolated from a pool of EMS-mutagenized *H. influenzae* cells created in a search for genes that regulate competence development (3). The present study began by using the same strategy to select additional hypercompetence mutations from the same population. Wild-type cells growing at low cell density in rich medium do not express competence genes or take up DNA, so an EMS-mutagenized culture was incubated with DNA carrying a novobiocin-resistance allele and Nov^R transformants were selected. Screening of the rare transformants identified four additional strains with mutations that mapped to *sxy*; the alleles were named *sxy-2*, *sxy-3*, *sxy-4* and *sxy-5*. As shown in Figure 1, all four mutants demonstrated the same 50-fold to 500-fold increased transformation frequencies as the *sxy-1* mutant, during both log phase growth (A_{600} 0.2) and late-log phase growth (A_{600} 1.0). All mutants grew normally in rich medium (sBHI). In MIV starvation medium, mutants and wild-type cells survived equally well and transformed at equally high frequencies (right panel of Figure 1).

Sequencing revealed that each strain carried a distinct single-point mutation in *sxy*; these are shown in Figure 2A. The *sxy-2* mutation (G₁₀₂A) is a silent substitution in the coding region, 4 bp upstream of the site of the *sxy-1* mutation (G₁₀₆A, V₁₉I). The other three mutations are clustered outside the coding region, near the 5' end of the 51 nt UTR (*sxy-3*: C₁₄T; *sxy-4*: T₁₅C; *sxy-5*: G₁₆T).

Because these mutations did not alter the Sxy protein sequence, site-directed mutagenesis was used to confirm that no other mutations, either in *sxy* or elsewhere in the genome, were responsible for the hypercompetence phenotypes. As had been done for *sxy-1* (4), each of the four mutations was re-created in a *H. influenzae sxy* plasmid cloned in *E. coli*, and introduced into wild-type

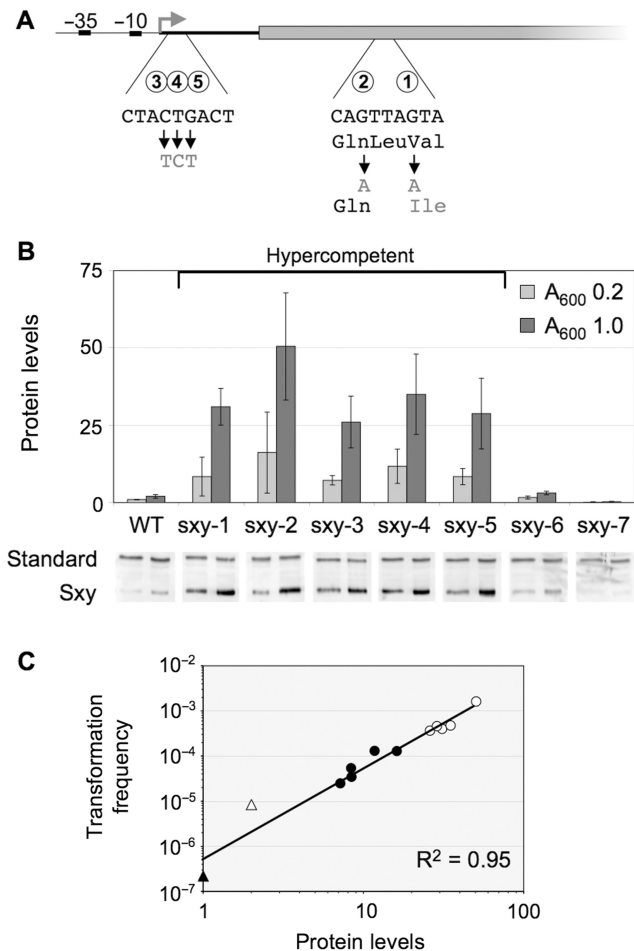


Figure 2. Analysis of Sxy levels in wild-type and mutant cells under different growth conditions. (A) Locations of key features and mutations in the *sxy* gene. Regulatory elements (-10, -35) are shown relative to the transcription start site (16). Sequences and circled numbers identify *sxy* hypercompetence mutations. (B) Quantitation of Sxy in wild-type and hypercompetent mutants in log (A_{600} 0.2) and late-log (A_{600} 1.0) growth. The average and standard deviation of four independent cultures are shown in the graph; protein levels are normalized to wild-type cells at A_{600} 0.2. The western blots below the graph show Sxy protein and an unidentified protein used for internal standardization (see Materials and Methods section). (C) Transformation frequencies as a function of Sxy protein levels for wild-type cells (triangles) and *sxy* hypercompetent mutants (circles), in sBHI at A_{600} 0.2 (filled symbols) and A_{600} 1.0 (open symbols).

H. influenzae chromosomes by transformation; these mutants all had phenotypes identical to the originals and were used in the experiments described here. This confirmed that all of the four new hypercompetence mutations increased competence without changing the sequence of Sxy or any other protein. We thus hypothesized that all five mutations acted by altering control of *sxy* expression rather than by changing Sxy function. As Sxy is an activator of competence genes, and as we observed elevated expression of all CRP-S regulon genes in microarray analysis of the *sxy-1* mutant in rich medium (data not shown), we predicted that the mutations would cause hypercompetence by increasing rather than decreasing *sxy* expression.

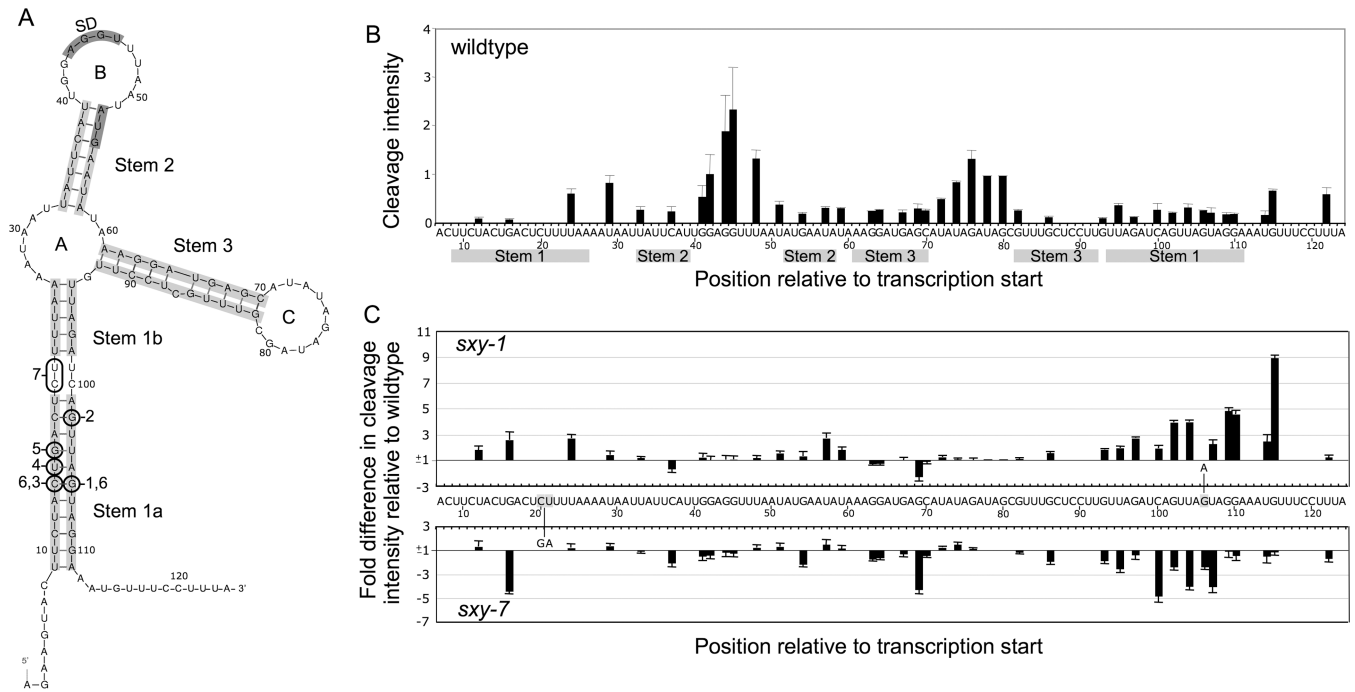


Figure 3. RNase analysis of *sxy* mRNA secondary structure. (A) Secondary structure predicted by Mfold. The Shine-Dalgarno site (SD) and start codon are shaded dark gray, and regions of predicted pairing are shaded light gray. Positions of *sxy* mutations are circled and numbered. (B) Cleavage intensity of *sxy* mRNA by single-strand-specific nucleases RNase A and RNase T1. Shaded bars correspond to stem regions shown in A. (C) Fold difference in cleavage intensity of mutant RNAs relative to wild type. Examples of gels used for this analysis are provided in Supplementary Figure 3.

Hypercompetence mutations lead to elevated Sxy under non-inducing and semi-inducing conditions

To compare Sxy levels between wild-type and mutant cells, we generated polyclonal anti-Sxy antibodies and used western blot analysis to quantify protein levels. In exponential growth (A_{600} 0.2), all hypercompetence mutants (*sxy-1-5*) had elevated Sxy levels, with 7- to 16-fold more protein than wild-type cells (Figure 2B; light gray bars). In late-log phase (A_{600} 1.0), the difference was even more striking, with mutants having 13- to 25-fold more Sxy protein than wild-type cells (Figure 2B, dark gray bars). Figure 2C graphs transformation frequencies as a function of Sxy protein levels for wild-type and mutant cells in the log and late-log phases of growth. The strong positive correlation between Sxy abundance and transformation frequencies confirms that Sxy levels limit competence development during growth in rich medium, and that changes in the amount of Sxy are responsible for the hypercompetence of the *sxy* mutants.

How do the *sxy-1-5* mutations cause increased Sxy production? Their locations rule out several possible modes of action. The mutations do not improve the affinity of the core promoter elements (-10 and -35 sequences), nor create a more efficient start codon or Shine-Dalgarno (SD) sequence, so they are unlikely to act by changing factors that determine baseline expression. The transformation frequencies and Sxy levels of the *sxy-1-5* mutants increase as the culture medium becomes exhausted, so the mutations must change the sensitivity

of the inducing mechanism rather than ablating repression. The mutations are unlikely to act by changing the binding site for a transcription factor, as they are outside of the promoter and spread over 94bp of transcript sequence.

The clustering of the mutations into two regions suggested that mRNA secondary structure might play a role in regulation. Examination of *sxy* mRNA for possible base pairing between these regions revealed a long stretch of potential base pairing between positions 9-26 of the UTR and positions 94-111 of the coding region, with only a single 2 x 2 bubble. All five hypercompetence mutations fall within this predicted stem. Moreover, each of the mutations eliminates a base pair within this stem, so that each is expected to destabilize the secondary structure. Analysis of this region with the RNA-folding program Mfold supported this folding model, and also predicted pairing between segments internal to this stem, creating two additional stems and three loops, as shown in Figure 3A.

Mfold analysis predicted the same optimal topology for *sxy-1-5* mRNAs as for wild-type mRNAs, but the *sxy-1-5* structures were not as thermodynamically stable and were predicted to have higher frequencies of single strandedness throughout. Supplementary Figure 2A plots the stability of Stem 1 in hypercompetent mutants, calculated by Mfold, showing that each point mutation is predicted to reduce the stability of Stem 1. In addition, this analysis predicts that Stem 1 will be the most important contributor to the overall stability of the

mRNA secondary structure, and thus may help explain why all five hypercompetence mutations were found in this region. Supplementary Figure 2B presents the analysis of single-strandedness across multiple thermodynamically stable folding predictions for the bases in Stem 1. The *sxy* point mutations are predicted to cause 2- to 3-fold increases in single-strandedness.

Nuclease mapping confirms the predicted *sxy* mRNA secondary structure

Nuclease mapping was used to test whether *sxy* mRNA folds into the predicted secondary structure *in vitro*, and to test whether hypercompetence mutations alter RNA folding. We first examined cleavage of wild-type *sxy* RNA by the structure-specific ribonucleases RNase T1 and RNase A, using a cloned *sxy* fragment extending from base 1 to base 323. RNase T1 cuts specifically at single-stranded Gs, while RNase A cuts single-stranded Cs and Us. Figure 3B shows the cleavage intensities of all scorable positions between positions 1 and 122, normalized to positions 78 and 80, which were consistently cleaved. (Data for some Cs and Us are not shown because they were not cut by RNase A even when the RNA was denatured.) The strong cleavages between positions 42 and 48, and between positions 72 and 80, confirm that Loops B and C form *in vitro*, and that they are separated by segments that are protected by pairing. The moderate cleavage at position 29 is consistent with the presence of Loop A. Only three positions in the upstream side of Stem 1 are informative; positions 12 and 16 are protected but position 24 is moderately cleaved, suggesting that Stem 1b may be weak. (Cleavage of position 24 could also be explained by a slight modification to the predicted pairing, with nucleotide 24 bulged out and the 3 nt below it shifted up one in their pairings.) The segment that forms the downstream side of Stem 1 (94–111) has more informative positions; these are consistently protected.

The nuclease-assay support for Stems 2 and 3 and Loops B and C suggests that the *sxy* SD site and start codon may be sequestered within a small loop and stem, respectively, likely preventing the initiation of translation. The biochemical evidence for Stem 1 is fairly strong, with most of the informative positions protected from cleavage. Importantly, of the sites of the five hypercompetence mutations, the three that are scorable in these assays are all strongly protected, supporting the hypothesis that they normally are paired.

We then examined mutant *sxy-1* RNA for changes in secondary structure; Figure 3C (upper panel) shows the effect of this single mutation. Note that this figure shows ratios of *sxy-1* cleavages to cleavages of wild-type *sxy* RNAs, not absolute intensities, so that bars above the line represent positions with increased nuclease sensitivity. The expected moderate destabilization of Stem 1a by the loss of base pairing between positions 14 and 106 is confirmed by the increased cleavage of positions 12 and 16 and positions 102–110. Modest increases in nuclease sensitivity were also seen in Stem 1b (position 24) and

Stem 2 (positions 57 and 59), and position 115 was very strongly cleaved.

Mutations that strengthen Stem I reduce *sxy* expression

The definitive test of whether a mutant phenotype results from disruption of base pairing is creation of compensatory mutations that restore the hypothesized base pairing. The test is especially clear here, as the *sxy-1* and *sxy-3* mutations make complementary substitutions disrupting the same proposed base pair. If both do increase *sxy* expression by destabilizing the secondary structure, then a double mutant carrying both substitutions will have base pairing restored and thus will have a more normal phenotype (lower competence) than either single mutant, rather than the more extreme phenotype expected if the mutations increase expression in some other way. The desired double mutant, *sxy-6*, was created by site-directed mutagenesis in *E. coli*, followed by transformation into the *H. influenzae* chromosome. This combined the *sxy-1* and *sxy-3* mutations to generate an A:U pair where wild-type *sxy* has a G:C pair (Figure 3A). Figure 2B shows that *sxy-6* cells produced wild-type levels of Sxy protein, much less than either parent mutant, confirming that the *sxy-1* and *sxy-3* mutations act by disrupting base pairing. The altered sequence but wild-type phenotype of the *sxy-6* mutant is strong evidence that the single mutant phenotypes are not due to sequence-dependent interactions with a regulatory protein or RNA.

To further characterize the ability of base pairing to limit *sxy* expression, a second mutant with enhanced base pairing was constructed. In *sxy-7*, two adjacent substitutions (C₂₀G and U₂₁A) create two new base pairings at the site of the 2 × 2 bubble separating Stems 1a and 1b (Figure 3A), so Stem 1 of *sxy-7* has 18 contiguous base pairings. Figure 3C (lower panel) shows that this change strongly reduced RNase cleavages at positions 16 and 102–107 (Stem 1b), 37 and 54 (Stem 2), 69 and 86 (Stem 3) of the RNA (again the values are relative to those in Figure 3B); the generally decreased cleavage in the entire region indicates stronger base pairing throughout. As expected, C₁₀₀, the predicted pairing partner of what is now G₂₀, was not cleaved. Sxy protein was barely detectable in this mutant (Figure 2B) and cells could not be transformed even after transfer to MIV (data not shown). Together the *sxy-6* and *sxy-7* mutations confirm that base pairing in Stem 1 limits *sxy* expression and competence development.

How does mRNA secondary structure regulate *sxy* expression?

In principle, the secondary structure of *sxy* mRNA could limit production of Sxy protein by interfering with elongation of transcription or by reducing the resulting mRNA's stability or translation efficiency. As described below, two independent methods (measurements of β -galactosidase production from *sxy::lacZ* fusions and direct measurements of *sxy* RNA and protein levels) both showed that the structure affects both accumulation and translation of *sxy* mRNA.

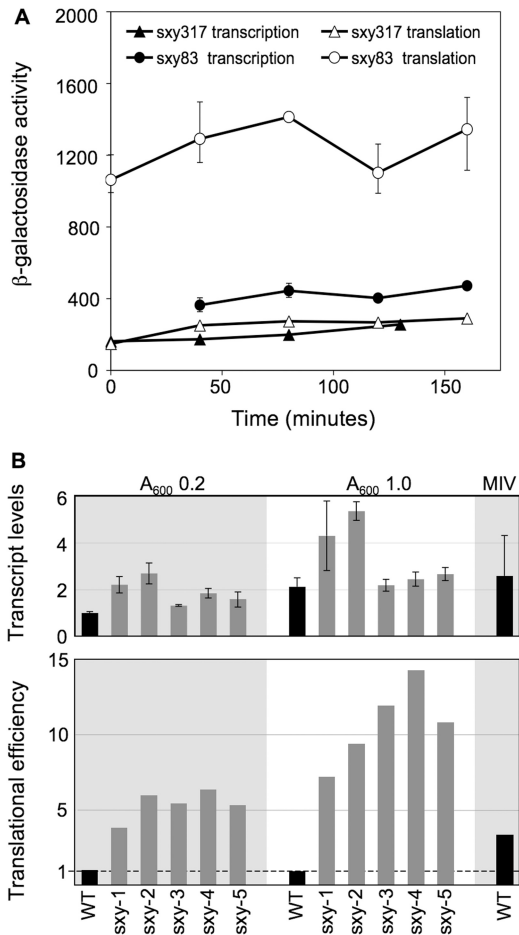


Figure 4. Effect of *sxy* mutations on *sxy* mRNA levels and translation efficiency. (A) Expression from *sxy::lacZ* transcriptional and translational fusions. Triangles, fusions to *sxy* position 317; circles, fusions to *sxy* position 83. Filled symbols, transcriptional fusions; open symbols, translational fusions. Each point is the mean of two replicate cultures. Error bars representing the range of the replicates are shown only where the range was ≥ 100 Miller units. The A_{600} of each sBHI culture increased from 0.085 to ~ 1.2 over the course of the experiments (i.e. cells divided 3–4 times). (B) Translational efficiency of *sxy* transcripts *in vivo*. Wild-type cells, black bars; hypercompetent mutants, gray bars. (upper panel) *sxy* mRNA levels measured using real-time PCR; error bars represent the range of levels from two or more independent cultures. (lower panel) *In vivo* translation efficiencies of these transcripts, calculated as the ratios of the protein levels in Figure 2 to the mRNA levels in the upper panel and normalized to wild-type cells at A_{600} 0.2.

The relative impacts of the *sxy* secondary structure on transcription and translation were first investigated using transcriptional and translational fusions of positions 83 and 317 of the wild-type *sxy* sequence to the *E. coli lacZ* gene (Figure 4A). The position 317 fusions maintain all of the secondary structure shown in Figure 3A. The position 83 fusions eliminate the downstream strands of Stems 1 and 3 and thus eliminate these stems. Full characterization of these and related *lacZ* fusions is provided by reference 14.

Expression from the *sxy317* transcriptional fusion (black triangles) revealed that transcription from the *sxy* promoter is quite stable during exponential growth

and early stationary phase in rich medium. The absence of the *lacZ* translation start site in the corresponding translational fusion (white triangles) did not significantly change the amount of β -galactosidase activity produced, indicating that the *sxy* and *lac* translation start sites have comparable activities. Elimination of Stems 1 and 3 in the *sxy83* transcriptional fusion increased expression 2-fold (black circles). The 5-fold increase in expression from the corresponding translational fusion (white circles) therefore represents a 2.5-fold increase in the amount of protein produced from each mRNA.

A parallel experiment directly tested whether the increased Sxy protein in hypercompetence mutants results from changes in accumulation and/or translation of *sxy* mRNA. Figure 4B plots mRNA abundance measured by quantitative PCR (upper panel), and the corresponding translational efficiencies (lower panel) calculated for wild-type cells and hypercompetent mutants from the protein levels in Figure 2B. Although hypercompetent mutants in early log produced 7- to 16-fold more protein than wild-type cells, they produced only slightly more mRNA, indicating that mutant translational efficiencies were elevated 3.5- to 6.5-fold. When wild-type cells entered late-log growth, the amount of *sxy* transcript and Sxy protein both doubled, so the translational efficiency did not change. However, when the hypercompetent mutants entered late log they showed an even greater disproportion between mRNA and protein than in early log, implying a greater increase in translational efficiency. Transfer of exponentially growing wild-type cells to MIV resulted in a 2.5-fold increase in the amount of *sxy* mRNA and a 9-fold increase in protein after 90 min, implying a 3.5-fold increase in translational efficiency. These results suggest that transfer to MIV maximizes competence in wild-type cells because it releases the translation limitation caused by mRNA secondary structure in rich medium.

mRNA secondary structure impedes translation *in vitro*

We used an *in vitro* coupled transcription/translation system to directly test the influence of mRNA secondary structure on the translation efficiency of *sxy* transcripts. Reactions were carried out at 25°C because this temperature reduces the transcription rate of T7 RNAP to a rate comparable to bacterial RNAP at 37°C, allowing nascent RNAs to fold correctly (15). All input DNAs (wild-type, *sxy-1* and *sxy-7* alleles) produced indistinguishable amounts of mRNA from the T7 promoter (data not shown), but wild-type and mutant mRNAs produced very different amounts of Sxy protein (Figure 5A). Spot-blot quantification of Sxy protein levels revealed that *sxy-1* mRNA was translated 3-fold more efficiently than wild-type mRNA, whereas *sxy-7* mRNA was translated about 4-fold less efficiently than wild-type mRNA.

We also tested whether a ssDNA oligonucleotide complementary to nucleotides 2–19 in Stem 1a (see inset of Figure 5B) could compete with formation of *sxy* mRNA secondary structure and thus improve translation efficiency. The oligonucleotide was designed to hybridize

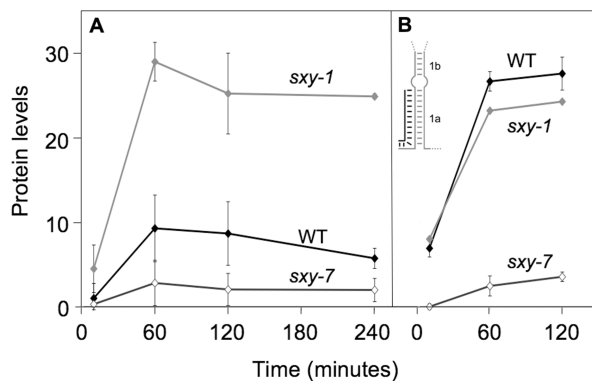


Figure 5. Sxy protein generated by *in vitro* transcription/translation. (A) Protein production from wild-type (WT), *sxy-1* and *sxy-7* DNA templates. The average and standard deviation of three independent time courses are shown. (B) Protein production in reactions containing a ssDNA oligonucleotide complementary to the 5'-end of *sxy* mRNA. The inset illustrates the oligonucleotide (black) binding to nucleotides 2–19 of the *sxy* transcript (gray), thus directly competing with formation of Stem 1a. The average and standard deviation of two independent time courses using WT and *sxy-7* template, and one time course using *sxy-1* template are shown. All Sxy protein levels are normalized to wild type at 10 min in (A).

with the 5'-terminus of *sxy*, *sxy-1* and *sxy-7* mRNAs, allowing it to compete with formation of Stem 1a (the location of all 5 hypercompetence mutations) without interfering with ribosome binding to the SD (Figure 3A). Figure 5B shows that inclusion of the oligonucleotide in reaction mixtures allowed wild-type mRNA to be translated as efficiently as *sxy-1* mRNA, but had no significant effect on the translatability of *sxy-1* or *sxy-7* mRNA. These results suggest that, *in vitro*, secondary structure does not inhibit translation of *sxy-1* mRNA. Conversely, the high stability of the *sxy-7* mRNA secondary structure not only prevents translation but also prevents competition of Stem 1a by the complementary oligonucleotide. The ability of this oligonucleotide to increase translation of wild-type *sxy* mRNA confirms that the wild-type secondary structure is strong enough to inhibit translation but sufficiently labile to respond to changing conditions.

CRP and cAMP strongly induce *sxy* transcription

Zulty and Barcak reported that the *sxy* promoter contained two CRP-binding sites, one centered at -5.5 and one at -61.5 relative to the transcription start point, and that *sxy* expression in rich medium was CRP-dependent (16). However the site they reported at -5.5 (overlapping the transcription start site) was created by an A \rightarrow G substitution at position -12 , and the authentic sequence of this site (17) (also confirmed in our lab) has no significant resemblance to known *H. influenzae* CRP sites (2). The site centered at -61.5 scored as an excellent CRP site when tested for goodness-of-fit with 58 experimentally determined *H. influenzae* CRP sites, as previously described (1), and is at the optimal position to activate transcription through a class I mechanism (18).

To test whether CRP induces and/or represses *sxy* in starvation medium (MIV), we measured *sxy* transcript

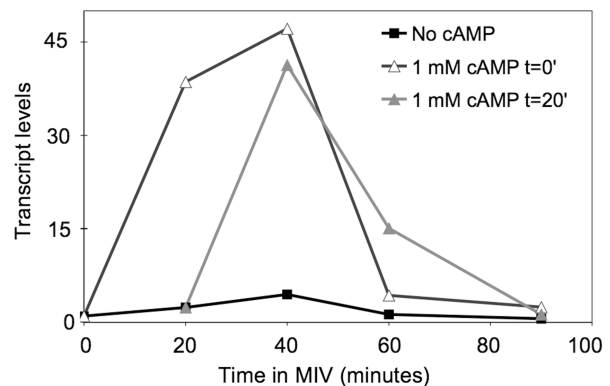


Figure 6. Control of *sxy* transcription by cAMP–CRP. RR668 cells (*cyaA*[−]) at A₆₀₀ 0.2 in sBHI were transferred to MIV, with 1 mM cAMP added at $t = 0'$ or $t = 20'$. *sxy* transcript was measured using real-time PCR.

levels in a *cyaA*[−] mutant that cannot synthesize CRP's allosteric effector cAMP (Figure 6). Transcription was induced only slightly in a *cyaA*[−] mutant. Adding 1 mM cAMP resulted in very strong induction of *sxy*, indicating that CRP does activate the *sxy* promoter. The promoter could be induced by cAMP added after 20 min in MIV, but the amount of *sxy* transcript still fell back to pre-induction levels after 40 min in MIV. Thus, CRP is a strong inducer of *sxy* expression, but continuing expression appears to be overridden by a repressing mechanism after 40 min. This mechanism is unlikely to be auto-repression of the *crp* gene by CRP, because *sxy* repression did not depend on when cAMP was added.

DISCUSSION

We have identified and characterized an extensive 5' stem-loop structure in the *sxy* transcript, which negatively regulates this competence-inducing transcription factor. Mutations that destabilize the secondary structure increase both the amount of *sxy* mRNA and the efficiency of its translation, causing greatly elevated competence under otherwise non-inducing conditions. These large phenotypic effects arise from minor perturbations in mRNA secondary structure; a mutation decreasing by one the number of base pairs in Stem 1 (*sxy-1*) destabilizes the structure while one increasing the number of base pairs by two (*sxy-7*) stabilizes folding.

In some mRNAs, secondary structure regulates expression by forming riboswitches or by preventing degradation by the single-strand-specific endoribonuclease RNase E (19,20), but these are unlikely to contribute to post-transcriptional regulation of *sxy* mRNA. The *sxy* secondary structure has no similarities to the well-conserved structures of known riboswitches (19). A role for RNase E can also be ruled out because weakening the secondary structure led to elevated transcript levels, contrary to the expectation if RNase E targets the *sxy* transcript.

The increased translation efficiency of *sxy* mutants with weakened mRNA secondary structure is most readily

explained by a simple model in which the secondary structure of wild-type mRNA limits ribosome binding. Ribosomes require that a 35–50 nt segment including the SD site be free of stable secondary structure (21). Indeed, extensive regions of double-stranded RNA at or near the SD site and start codon, like the secondary structure we have detected in *sxy* mRNA, are known to preclude ribosome binding to (and consequently translation of) several bacterial mRNAs (22–25). Under this model of *sxy* expression, the moderate increase in transcript abundance in the *sxy83* transcriptional fusion strain (Figure 4A) and in hypercompetent mutants (Figure 4B) arises because mutant mRNAs are more often occupied by ribosomes and thus protected from degradation [see (26) for a recent review of ribosome protection], rather than because hypercompetence mutations activate the *sxy* promoter. Furthermore, use of a T7 promoter to generate *sxy* mRNA for *in vitro* translation confirmed that the hypercompetence phenotype can be explained primarily by improved translation efficiency and not by mutational effects on *sxy*'s native promoter.

The rise in the ratio of *sxy* protein to mRNA induced by transfer to MIV starvation medium suggests that the secondary structure does more than establish a baseline level of translation. Rather, it has the potential to play a sensory role that explains the repression of competence by purine nucleotides (27). In bacteria, multiple regulatory mechanisms link nucleotide availability to transcription initiation, promoter escape and elongation (28–32). For example, translation of *E. coli*'s pyrimidine biosynthesis operon *pyrBI* is contingent on nucleotide starvation (33). When cells are starved for the pyrimidine nucleotide UTP, transcription pausing in the *pyrBI* leader sequence allows ribosome loading to prevent folding of an mRNA-terminating hairpin (34).

However, unlike the small *pyrBI* terminator hairpin (~20 nt), the >100 nt *sxy* mRNA structure allows two other kinetic factors to come into play. First, large mRNA secondary structures require time to fold after their synthesis is complete, especially if the final structure involves pairing between non-adjacent segments as in Stem 1 of *sxy* mRNA (35). Translation thus may initiate more easily on newly synthesized transcripts than on ones that have had time to fold. Even so, the ability of an oligonucleotide to compete with the secondary structure of *sxy*, but not *sxy-7* indicates that double-stranded regions of the wild-type transcript are sufficiently dynamic to allow invasion by more stable partners (Figure 5B), suggesting that *sxy* mRNA secondary structure never completely precludes ribosome binding.

A more important contribution to regulation may come from a second kinetic factor: the distance RNAP must transcribe between synthesis of the translation initiation signals (SD and start codon) and synthesis of the downstream portion of the secondary structure that would block access to them. In *sxy* mRNA this distance is 60 nt. Dynamic modeling of *sxy* mRNA folding using the RNA Kinetics server (<http://www.ig-msk.ru/RNA/kinetics/>) predicted that the segment of *sxy* mRNA containing the SD site and the start codon will remain

largely unstructured until more than 100 nt have been synthesized. The availability of this potential landing platform for ribosomes will in turn depend on the rate of transcription, thus making the progress of RNA polymerase a potential transducer of nutritional signals.

Nucleotide pools are not limiting to *H. influenzae* during growth in rich medium, so the resulting rapid transcription may allow *sxy* mRNA to usually fold before ribosomes load. Under these conditions, translation may only be able to initiate during rare unfolding events, consistent with the dramatic effects in rich medium of the *sxy-1-5* mutations that decrease thermodynamic stability. Transfer to MIV causes abrupt depletion of nucleotide pools, and the resulting slowing of transcription may be sufficient to allow translation to initiate on most nascent wild-type transcripts. The combination of increased translation efficiency with the increased transcription caused by rising cAMP would then lead to a burst of Sxy production, followed by expression of competence genes.

Sxy is not the only regulator of competence in MIV; CRP activity at the CRP-S promoters of competence genes is known to be elevated because MIV-treated cells produce more cAMP than cells in rich medium (36). Consistent with this, wild-type cells in MIV produce less Sxy protein but become more competent than hypercompetent mutants in rich medium. In addition, at least one essential competence gene has a candidate PurR-binding site in its promoter, and PurR repression of purine biosynthesis genes is relaxed in MIV (2). We are currently testing whether PurR represses competence when nucleotide pools are high. Understanding the interplay of signals transduced by CRP/cAMP, Sxy and possibly PurR will clarify how nutritional sensing controls DNA uptake.

SUPPLEMENTARY DATA

Supplementary Data are available at NAR Online.

ACKNOWLEDGEMENTS

We thank Qing Qian and Caixia Ma for technical support, and George Mackie, Kristian Baker, George Spiegelman, Brett McLeod and Arina Omer for technical advice. This work was supported by an Operating Grant from the Canadian Institutes for Health Research to R.J.R. Funding to pay the Open Access publication charges for this article was provided by the Canadian Institute of Health Research.

Conflict of interest statement. None declared.

REFERENCES

1. Cameron, A.D. and Redfield, R.J. (2006) Non-canonical CRP sites control competence regulons in *Escherichia coli* and many other gamma-proteobacteria. *Nucleic Acids Res.*, **34**, 6001–6014.
2. Redfield, R.J., Cameron, A.D., Qian, Q., Hinds, J., Ali, T.R., Kroll, J.S. and Langford, P.R. (2005) A novel CRP-dependent regulon controls expression of competence genes in *Haemophilus influenzae*. *J. Mol. Biol.*, **347**, 735–747.

3. Redfield, R.J. (1991) *sxy-1*, a *Haemophilus influenzae* mutation causing greatly enhanced spontaneous competence. *J. Bacteriol.*, **173**, 5612–5618.
4. Williams, P.M., Bannister, L.A. and Redfield, R.J. (1994) The *Haemophilus influenzae sxy-1* mutation is in a newly identified gene essential for competence. *J. Bacteriol.*, **176**, 6789–6794.
5. Bhattacharjee, M.K., Fine, D.H. and Figurski, D.H. (2007) *tfoX* (*sxy*)-dependent transformation of *Aggregatibacter* (*Actinobacillus*) *actinomycetemcomitans*. *Gene*, **399**, 53–64.
6. Meibom, K.L., Blokesch, M., Dolganov, N.A., Wu, C.Y. and Schoolnik, G.K. (2005) Chitin induces natural competence in *Vibrio cholerae*. *Science*, **310**, 1824–1827.
7. Postma, P.W., Lengeler, J.W. and Jacobson, G.R. (1996) Phosphoenolpyruvate:carbohydrate phosphotransferase system. In Neidhardt, F.N. *et al.* (eds), *Escherichia coli and Salmonella typhimurium*, Vol. II. ASM Press, Washington, DC, pp. 1149–1174.
8. Macfadyen, L.P., Ma, C. and Redfield, R.J. (1998) A 3',5' cyclic AMP (cAMP) phosphodiesterase modulates cAMP levels and optimizes competence in *Haemophilus influenzae* Rd. *J. Bacteriol.*, **180**, 4401–4405.
9. Poje, G. and Redfield, R.J. (2003) Transformation of *Haemophilus influenzae*. *Methods Mol. Med.*, **71**, 57–70.
10. Poje, G. and Redfield, R.J. (2003) General methods for culturing *Haemophilus influenzae*. *Methods Mol. Med.*, **71**, 51–56.
11. Ausubel, F.M. (1995) *Current Protocols in Molecular Biology*. J. Wiley & Sons, Inc, Brooklyn, NY.
12. Zuker, M. (2003) Mfold web server for nucleic acid folding and hybridization prediction. *Nucleic Acids Res.*, **31**, 3406–3415.
13. Miller, J.H. (1992) *A Short Course in Bacterial Genetics: a Laboratory Manual and Handbook for Escherichia coli and Related Bacteria*. Cold Spring Harbor Laboratory Press, Plainview, N.Y.
14. Bannister, L.A. (1999) An RNA secondary structure regulates *sxy* expression and competence development in *Haemophilus influenzae*. *Ph.D. Thesis*. University of British Columbia.
15. Lewicki, B.T., Margus, T., Remme, J. and Nierhaus, K.H. (1993) Coupling of rRNA transcription and ribosomal assembly in vivo. Formation of active ribosomal subunits in *Escherichia coli* requires transcription of rRNA genes by host RNA polymerase which cannot be replaced by bacteriophage T7 RNA polymerase. *J. Mol. Biol.*, **231**, 581–593.
16. Zulty, J.J. and Barcak, G.J. (1995) Identification of a DNA transformation gene required for *com101A+* expression and supertransformer phenotype in *Haemophilus influenzae*. *Proc. Natl Acad. Sci. USA*, **92**, 3616–3620.
17. Fleischmann, R.D., Adams, M.D., White, O., Clayton, R.A., Kirkness, E.F., Kerlavage, A.R., Bult, C.J., Tomb, J.F., Dougherty, B.A. *et al.* (1995) Whole-genome random sequencing and assembly of *Haemophilus influenzae* Rd. *Science*, **269**, 496–512.
18. Lawson, C.L., Swigon, D., Murakami, K.S., Darst, S.A., Berman, H.M. and Ebright, R.H. (2004) Catabolite activator protein: DNA binding and transcription activation. *Curr. Opin. Struct. Biol.*, **14**, 10–20.
19. Mandal, M. and Breaker, R.R. (2004) Gene regulation by riboswitches. *Nat. Rev. Mol. Cell Biol.*, **5**, 451–463.
20. Cohen, S.N. and McDowall, K.J. (1997) RNase E: still a wonderfully mysterious enzyme. *Mol. Microbiol.*, **23**, 1099–1106.
21. de Smit, M.H. and van Duin, J. (2003) Translational standby sites: how ribosomes may deal with the rapid folding kinetics of mRNA. *J. Mol. Biol.*, **331**, 737–743.
22. Carter-Muenchau, P. and Wolf, R.E. (1989) Growth-rate-dependent regulation of 6-phosphogluconate dehydrogenase level mediated by an anti-Shine-Dalgarno sequence located within the *Escherichia coli* *gnd* structural gene. *PNAS*, **86**, 1138–1142.
23. de Smit, M.H. and van Duin, J. (1990) Control of prokaryotic translational initiation by mRNA secondary structure. *Prog. Nucleic Acid Res. Mol. Biol.*, **38**, 1–35.
24. de Smit, M.H. and van Duin, J. (1994) Control of translation by mRNA secondary structure in *Escherichia coli*. A quantitative analysis of literature data. *J. Mol. Biol.*, **244**, 144–150.
25. Kozak, M. (2005) Regulation of translation via mRNA structure in prokaryotes and eukaryotes. *Gene*, **361**, 13–37.
26. Deana, A. and Belasco, J.G. (2005) Lost in translation: the influence of ribosomes on bacterial mRNA decay. *Genes Dev.*, **19**, 2526–2533.
27. MacFadyen, L.P., Chen, D., Vo, H.C., Liao, D., Sinotte, R. and Redfield, R.J. (2001) Competence development by *Haemophilus influenzae* is regulated by the availability of nucleic acid precursors. *Mol. Microbiol.*, **40**, 700–707.
28. Walker, K.A., Mallik, P., Pratt, T.S. and Osuna, R. (2004) The *Escherichia coli* *Fis* promoter is regulated by changes in the levels of its transcription initiation nucleotide CTP. *J. Biol. Chem.*, **279**, 50818–50828.
29. Schneider, D.A., Gaal, T. and Gourse, R.L. (2002) NTP-sensing by rRNA promoters in *Escherichia coli* is direct. *Proc. Natl Acad. Sci. USA*, **99**, 8602–8607.
30. Uptain, S.M., Kane, C.M. and Chamberlin, M.J. (1997) Basic mechanisms of transcript elongation and its regulation. *Annu. Rev. Biochem.*, **66**, 117–172.
31. Qi, F. and Turnbough, C.L.J. (1995) Regulation of *codBA* operon expression in *Escherichia coli* by UTP-dependent reiterative transcription and UTP-sensitive transcriptional start site switching. *J. Mol. Biol.*, **254**, 552–565.
32. Cheng, Y., Dylla, S.M. and Turnbough, C.L.J. (2001) A long T. A tract in the *upp* initially transcribed region is required for regulation of *upp* expression by UTP-dependent reiterative transcription in *Escherichia coli*. *J. Bacteriol.*, **183**, 221–228.
33. Turnbough, C.L., Hicks, K.L. and Donahue, J.P. (1983) Attenuation control of *pyrBI* operon expression in *Escherichia coli* K-12. *Proc. Natl Acad. Sci. USA*, **80**, 368–372.
34. Donahue, J.P. and Turnbough, C.L.J. (1994) Nucleotide-specific transcriptional pausing in the *pyrBI* leader region of *Escherichia coli* K-12. *J. Biol. Chem.*, **269**, 18185–18191.
35. Groeneveld, H., Thimon, K. and van Duin, J. (1995) Translational control of maturation-protein synthesis in phage MS2: a role for the kinetics of RNA folding? *RNA*, **1**, 79–88.
36. Macfadyen, L.P. (1999) PTS regulation of competence in *Haemophilus influenzae*. *Ph.D. Thesis*. University of British Columbia.
37. Alexander, H.E. and Leidy, G. (1951) Determination of inherited traits of *H. influenzae* by desoxyribonucleic acid fractions isolated from type-specific cells. *J. Exp. Med.*, **93**, 345–359.
38. Barcak, G.J., Chandler, M.S., Redfield, R.J. and Tomb, J.F. (1991) Genetic systems in *Haemophilus influenzae*. *Methods Enzymol.*, **204**, 321–342.
39. Dorocicz, I.R., Williams, P.M. and Redfield, R.J. (1993) The *Haemophilus influenzae* adenylate cyclase gene: cloning, sequence, and essential role in competence. *J. Bacteriol.*, **175**, 7142–7149.